Various effects of AAV9-mediated βARKct gene therapy on the heart in dystrophin-deficient (*mdx*) mice and δ-sarcoglycan-deficient (*Sgcd-/-*) mice

Ralf Bauer[a,*], Helene Enns[a], Andreas Jungmann[a], Barbara Leuchs[c], Christian Volz[a], Stefanie Schinkel[a], Walter J. Koch[d], Philip W. Raake[a,b], Patrick Most[a,b,e], Hugo A. Katus[a,b], Oliver J. Müller[a,b,f]

[a] *Internal Medicine III, University Hospital Heidelberg, Im Neuenheimer Feld 410, 69120 Heidelberg, Germany*
[b] *DZHK (German Center for Cardiovascular Research), Partner Site Heidelberg/Mannheim, Germany*
[c] *Tumor Virology, German Cancer Research Center, Im Neuenheimer Feld 580, 69120 Heidelberg, Germany*
[d] *Center for Translational Medicine, Temple University School of Medicine, 3500 N Broad St, 19140 Philadelphia, PA, USA*
[e] *Center for Molecular and Translational Cardiology, University Hospital Heidelberg, Im Neuenheimer Feld 410, 69120 Heidelberg, Germany*
[f] *Department of Internal Medicine III, University of Kiel, Arnold-Heller-Str. 3, 24105 Kiel, Germany*

1. Introduction

Mutations in genes coding for major protein components of the cytoskeleton in heart and skeletal muscle cells clinically lead to a heterogeneous group of muscular dystrophies frequently associated with severe cardiomyopathy [1]. In Duchenne muscular dystrophy (DMD) and limb girdle muscular dystrophy type 2 F (LGMD2F), absence of dystrophin or δ-sarcoglycan (Sgcd) disrupts the dystrophin-glycoprotein-complex (DGC) progressively damaging cardiac and skeletal muscle cells [2]. In almost every patient with DMD or LGMD2F subclinical or clinical cardiomyopathy can be found with strong impact on mortality.

However, it remains unclear whether universally evidence based treatment strategies of heart failure are applicable to every causally distinct form of cardiomyopathy. The contribution of alterations in β-adrenergic receptor (βAR) signalling such as upregulation of G protein-coupled receptor kinase-2 (GRK2) in maintaining cardiac dysfunction in heart failure is well documented [3,4]. However, it is not well investigated in cardiomyopathies associated with muscular dystrophies. Likewise, although large studies have shown protective effects of β-blocker treatment in patients with heart failure [5], the benefit of these drugs in treating the specific subgroup

* Corresponding author.
E-mail addresses: ralf.bauer@wiesloch-zwei.de, ralf.bauer@med.uni-heidelberg.de (R. Bauer).

of patients with muscular dystrophy and cardiomyopathy is not yet established [6]. In a previous study we demonstrated a genotype-dependent response to pharmacological treatment with β-blockers, with beneficial effects in dystrophin-deficient *mdx* mice and rather harmful effects in Sgcd-deficient mice (*Sgcd -/-*) despite a functional interaction between dystrophin and the membrane-bound sarcoglycan complex [7]. In this earlier study the underlying pathophysiological mechanisms remained elusive, although the finding is clinically relevant with regard to the need of "individualized" treatment of patients with cardiomyopathy with or without muscle involvement. The distinct response pattern to pharmacological β-blockade indicates the need to develop more specific treatment strategies for patients with muscular dystrophy associated cardiomyopathy.

A promising approach to target maladaptive increase of GRK2 in heart failure represents a competitive inhibition of the GRK2-βAR-interaction through βARKct. βARKct is a polypeptide which consists of the last 194 C-terminal amino acid residies of GRK2 [8–10]. Although βARKct is effective also in other non-cardiac tissues such as vessels and nervous system so far no harmful side effects of βARKct-treatment were documented in previous studies [11,12]. Previously we found that in *mdx* mice GRK2 is upregulated whereas in *Sgcd-/-* mice GRK2 was not changed compared to wildtype mice. Therefore, we hypothesized that differences of GRK2 may lead to different βAR signaling in these two mouse models.

Therapeutic gene transfer of βARKct using adeno-associated virus (AAV)-vectors has been used for long-term, cardiac gene transfer in small and large animal models of heart failure and can significantly improve hemodynamic parameters and adverse ventricular remodelling [13,14]. The use of AAV vectors of serotype 9 enabled a highly efficient cardiac gene transfer after systemic application in mice making this vector system an ideal candidate for the study of novel gene therapeutic approaches in mouse models [15,16].

The aim of the present study was therefore to investigate the efficiency of an inhibition of GRK2 through AAV9-mediated cardiac overexpression of βARKct (*AAV9/ βARKct*) to prevent the development of cardiomyopathy in *mdx* and *Sgcd-/-* mice, established mouse models for DMD and LGMD2, respectively. We found that *AAV9/ βARKct* treatment particularly improved left ventricular function and ameliorated hypertrophy in dystrophin-deficient *mdx* mice. By contrast in *Sgcd-/-* mice beneficial effects on development of heart failure were mild without any protection from hypertrophy. Neither GRK2 nor nuclear factor-kappaB (NFκB) were upregulated in *Sgcd-/-* mice, potentially explaining the different therapeutic response in these mouse models.

2. Material and methods

2.1. Generation of the βARKct construct and AAV9 vectors

For human codon usage optimized βARKct-cDNA was generated (Geneart, Regensburg, Germany) and inserted into pdsCMV-MLC0.26-EGFP resulting in pdsCMV-MLC0.26-βARKct [17,18]. For production of AAV9/βARKct and AAV9/EGFP vectors, this plasmid was used for co-transfection of 293T cells together with p5E18-VD2-9, encoding the AAV-9 cap sequence, and pDGdelVP, containing the AAV-2 rep gene as well as adenoviral helper sequences [19,20]. AAV vectors were purified and titrated using SYBR green PCR with CMVenh329fwd (5′-TGCCCAGTACATGACCTTATGG-3′) as forward and CMVenh462rev (5′-GAAATCCCCGTGAGTCAAACC-3′) as reverse primer [21].

2.2. Animals and systemic in vivo vector delivery

Male *mdx* mice ($n=32$) and C57Bl/10 wildtype control mice ($n = 11$) were obtained as a gift from Prof. Dr. R. Fink (Institute of Physiology, University of Heidelberg). *Sgcd-/-* mice ($n = 28$) (B6.129-Sgcdtm1Mcn/J) were obtained from Jackson Laboratory (Bar Harbor, ME, USA) and bred in our animal facility. Wildtype littermates ($n = 10$) were used as controls for *Sgcd-/-* mice. Mice were housed under controlled temperature (17–28 °C) and light conditions (12:12 h light: dark cycle) and had free access to food and water. All procedures involving the use and care of animals were performed according to the Guide for the Care and Use of Laboratory Animals published by the US National Institutes of Health (NIH Publication No. 85–23, revised 1996) and the German animal protection code. Approval was also granted by the local ethics review board. 10^{12} viral genomes of AAV9 were injected into the tail vein of 8 weeks-old *mdx* ($n = 11$) and *Sgcd-/-* ($n = 10$) mice as a 150 µl bolus using a sterile 29-gauge needle. At the end of the study, animals were euthanized by cervical dislocation and hearts were rapidly frozen in liquid nitrogen after dissection. To control for potential side effects of high dose AAV9 vectors, further *mdx* ($n = 10$) and *Sgcd-/-* mice ($n = 8$) were injected with an AAV9/EGFP-vector. There were no differences between untreated and *AAV9/EGFP*-treated *mdx* mice in morphology and cardiac hemodynamics at the age of 12 months (Supplementary table).

2.3. Immunoblotting

Protein samples from hearts were homogenized in RIPA-buffer (with 0,1% SDS) (Roche) using a tissue lyser (MM301, Quiagen, Hilden, Germany). Lysates were cleared from cellular debris by centrifugation for 5 minutes at 13,000 rpm and a total amount of 50 µg of protein was loaded onto a 3–8% gradient gel (TRIS-glycine gel, Invitrogen, Karlsruhe, Germany). Protein was blotted on a PVDF membrane (Millipore, Billerica, USA) using βARKct and GRK2 (sc-562, C-15, rabbit, polyclonal, Santa Cruz Biotechnology, 1:5,000), phospho-NF-κB p65 (Ser536) (rabbit, monoclonal, Cell signaling technology) and Glycerinaldehyd-3-phosphat-Dehydrogenase (GAPDH) (clone 6C5, mouse, monoclonal, Millipore, Billerica, Massachusetts, USA, 1:20,000) as primary antibodies (directed against mouse, rat and chicken). A fluorophore

labeled goat anti rabbit (IRDye 800) and a goat anti mouse (IRDye 680, LI-COR, Lincoln, USA), diluted 1:10.000 in 1x Roti-Block, were used to visualize protein bands by Odyssey infrared imaging (LI-COR, Lincoln, USA). To perform relative quantification of the bands obtained by immunobloting, we applied ImageJ software based analysis (http://rsb.info.nih.gov/ij/). The area under curve (AUC) of the specific signal was corrected for the AUC of the loading control GAPDH. N =5 for all animal groups.

2.4. Real-time polymerase chain reaction

For analysis of mRNA expression levels of brain natriuretic peptide (BNP), the α-subunit of the stimulatory G-protein ($G_s\alpha$), phospholamban (pln) and sarcoplasmic reticulum Ca2+-ATPase (SERCA2A) total RNA was extracted from cardiac tissue lysates of untreated and *AAV9/βARKct*-treated *mdx*, *Sgcd-/-* and wild type control mice with the Rneasy Fibrous Tissue Mini Kit (Qiagen®, Hilden, Germany) (n = 8 each animal group). SuperScript III reverse transcriptase (Invitrogen, Karlsruhe, Germany) was used to randomly reverse transcribe 1 µg of RNA into cDNA according to the manufacturerś specifications. Quantitative real time PCR was performed on an ABI PRISM 7000 (Applied Biosystems, Foster City, USA) using QuantiTect primer assays (Qiagen®, Hilden, Germany; assay name/catalog numbers: BNP [Mm_Nppb_1_SG/QT00107541]; $G_s\alpha$ [Mm_Gnas_1_SG/QT00134127]; pln [Mm_Pln_1_SG/QT00254366]; SERCA2A [Mm_Atp2a2_1_SG/QT00149121]; GAPDH [Mm_Gapdh_3_SG/QT01658692]) and SYBR GreenER qPCR SuperMix (Invitrogen®, Karlsruhe, Germany). For detection of βARKct the primers *-forward: gga agt ggc cga gac cgt c and reverse: gct cat gta gcc gtg cat g-* were generated.

2.5. Histological analysis and determination of cardiomyocyte cross-sectional areas

Frozen 10 µm transverse sections were cut from the mid-part of hearts. To analyse cardiomyocyte cross-sectional areas color images were made of H&E-stained heart sections of untreated, *AAV9/βARKct*-treated *mdx*, *Sgcd-/-* and wildtype mice (n = 5 per group) at 20x total magnification using a Nikon Eclipse 90i upright automated microscope with a DS-Ri1 color camera (Nikon, Düsseldorf, Germany). For appropriate measurement of cardiomyocyte cross-sectional areas, sections were chosen which include the papillary muscles and microphotographs were taken from the area adjacent to the papillary muscles [[22] and supplemental Figure 1]. Images were opened in ImageJ and after setting the threshold 25 cardiomyoctes per animal were analysed.

Masson-Trichrome staining was performed to analyse fibrosis of heart sections of untreated, *AAV9/βARKct*-treated *mdx*, *Sgcd-/-* and wild type mice (n = 5 per group). Areas of fibrosis, appearing blue with Masson-Trichrome staining were highlighted, and the fibrotic area was analysed at 4x total magnification with Image J software and calculated in percentage area of fibrosis.

2.6. Transthoracic echocardiography

The ventral chest area of mice was depilated one day before echocardiography. For echocardiography, a Sonos 5500 (Philips, Eindhoven, NL) with a S12 transducer (12 MHz) was used and the performing person was blinded during procedure. To evaluate cardiac function, three consecutive beats were analysed to obtain the left ventricular end-diastolic diameter (LVEDD) and the left ventricular end-systolic diameter (LVESD). Cardiac function is represented as fractional shortening (FS) which was calculated as FS % = [(LVEDD-LVESD)/LVEDD] x 100. The thickness of left ventricular posterior wall was measured in diastole (PWTd) (number of animals examined s. Table 1).

2.7. Pressure volume (PV) loops

Measurements were made in closed-chest, spontaneously breathing mice (number of animals examined s. Table 1). Mice were anaesthetized by intraperitoneal injection of Medetomidin (0,5 µg/g body weight), Fentanyl (0,05 µg/g body weight) and Midazolam (5 µg/g body weight). Body temperature was maintained at 37 °C using a homoeothermic blanket (Harvard apparatus Ltdw, Edenbridge, UK). A 1.2 Fr catheter (Model FT111B Scisense Inc., London, ON, Canada) was inserted into the left ventricle of the mouse through the carotid artery to simultaneously measure pressure and volumes. Left ventricular volumes were extrapolated from admittance magnitude and admittance phase in real time using the ADVantage PV system (Scisense Inc., London, ON, Canada).

Pressure and volume data were recorded using a Scisense 404–16 Bit Four Channel Recorder with LabScribe2 Software (Scisense Inc., London, ON, Canada). Indices of systolic function included end-systolic pressures (ESP), stroke volume (SV) and stroke work (SW). Load dependent myocardial contractility was assessed by maximal rate of pressure development (dP/dt_{max}). Transient inferior vena caval compressions were applied to reduce preload and determine end-systolic elastance (Ees) as a parameter of load-independent myocardial contractility as previously described [23]. Diastolic function was assessed by end-diastolic pressure (EDP), tau (Weiss method, regression of log of pressure vs. time) and the maximal rate of pressure decay (dP/dt_{min}). Left ventricular size was determined by end-diastolic volumes (EDV). Two *mdx* mice died during the procedure without obtaining any loops (number of animals examined s. Table 1). C57Bl/10 present higher left ventricular volumes compared to C57Bl/6 mice in our PV-loops experiments (Table 1).

2.8. Statistical analysis

For statistical analysis we used the GraphPad prism® software version 5.01. All data are presented as the mean ±

Table 1
Comparison of hemodynamic variables for untreated and *AAV9/βARKct*-treated *mdx* and *Sgcd-/-* mice and the corresponding wildtype control mice.

PV loops	C57Bl/10 (n=5)	*mdx* (n=6)	*Mdx*+βARKct (n=8)	C57/Bl/6 (n=8)	*Sgcd -/-* (n=8)	*Sgcd -/-*+βARKct (n=8)
HR (bpm)	458 (±12)	356 (±40)	410 (±17)	466 (±32)	403 (±17)	447 (±14)
ESP (mmHg)	125 (±3)	83 (±6)*	96 (±5)	109 (±6)	87 (±3)***	94 (±3)
Dp/dt_{max} (mmHg/s)	12,355 (±932)	5624 (±229)*	7607 (±210)**	11,385 (±661)	6436 (±361)***	7914 (±629)
SV (µl)	23 (±2)	9 (±1)*	18 (±1)**	18 (±1)	12 (±1)***	11 (±1)
SW (µl*mmHg)	3054 (±339)	768 (±234)*	1910 (±132)**	2061 (±150)	1141 (±120)***	1120 (±53)
Ees (mmHg/µl)	10,1 (±0,4)	4,8 (±0,7)*	9,9 (±2,1)**	8,9 (±1,9)	3,9 (±0,4)***	6,3 (±0,9)
EDV (µl)	40 (±4)	38 (±2)	35 (±4)	26 (±1)	37 (±1)***	33 (±1)
EDP (mmHg)	9 (±5)	8 (±3)	8 (±1)	7 (±0,7)	12 (±0,4)***	10 (±0,9)
Tau weiss (msec)	7,8 (±1,9)	11,4 (±1,4)*	8,1 (±0,6)	6,5 (±0,4)	9,1 (±0,4)***	7,2 (±0,3)
Dp/dt_{min} (mmHg/s)	−8257 (±1117)	−5469 (±551)*	−6510 (±288)	−9389 (±540)	−5394 (±330)***	−6859 (±414)
E_a (mmHg/µl)	9,8 (±2,3)	7,8 (±1,1)	7,6 (±1,2)	7,8 (±1,3)	8,1 (±2,3)	8,7 (±1,3)
Echocardiography	(n=5)	(n=11)	(n=11)	(n=10)	(n=10)	(n=10)
FS (%)	74 (±3)	49 (±4)*	65 (±2)**	60 (±2)	32 (±4)***	44 (±1)****
PWTd (mm)	1,1 (±0,07)	1,8 (±0,06)*	1,2 (±0,07)**	1,1 (±0,07)	1,0 (±0,07)	0,9 (±0,07)

Values presented as mean+[standard error].
HR, heart rates; ESP, end-systolic pressures; dP/dt_{max}, maximal rate of pressure development; SV, stroke volume; SW, stroke work; Ees, end-systolic elastance; dP/dt_{min}, maximal rate of pressure decay; E_a, arterial elastance; FS, fractional shortening.
* $p<0.05$ *mdx* untreated vs. C57Bl/10.
** $p<0.05$, *mdx* untreated vs. *mdx*+βARKct.
*** $p<0.05$ *Sgcd -/-* untreated vs. C57Bl/6.
**** $p<0.05$, *Sgcd -/-* untreated vs. *Sgcd -/-*+βARKct.

standard error. To test for statistical significance between groups, a one-way ANOVA with Bonferroni subgroup analysis was applied. If appropriate, Student's *t*-test was employed (two-sided). Tests for normal distribution of values were performed using the Shapiro–Wilk method. Error bars represent standard error (SEM). Differences in data were considered significant at $p < 0.05$.

3. Results

3.1. *Long-term cardiac βARKct transgene expression in* mdx *and* Sgcd-/- *mice*

We generated an AAV9 vector containing codon-optimised βARKct cDNA (*AAV9/βARKct*) under transcriptional control of the cardiac-specific CMV-MLC promoter (Fig. 1A). We injected this construct into mice at 8 weeks of age and followed them to 12 months of age. At the age of 12 months *AAV9/βARKct*- injected *mdx* and *Sgcd-/-* mice showed a similar expression of *βARKct* mRNA (Fig. 1B) following 10 months of treatment ($n = 8$ each group).

3.2. AAV9/βARKct-*treatment improves cardiac haemodynamic function in* mdx *and* Sgcd-/- *mice*

Cardiac function echocardiography was normal at the age of 8 weeks when treatment was started in *mdx* and *Sgcd-/-* mice (supplemental Figure 2 and Table 1). At the age of 6 months fractional shortening was significantly decreased only in *Sgcd-/-* mice compared to wildtype (supplemental Figure 2). At the age of 12 months, both *mdx* and *Sgcd-/-* mice had developed ventricular dysfunction (number of animals examined s. Table 1). Untreated *mdx* and *Sgcd-/-* mice showed compromised fractional shortening (FS) in echocardiography. Pressure volume loops revealed reduced myocardial contractility (dp/dt_{max} and end-systolic elastance (Ees)), decreased stroke volume (SV) and stroke work (SW) (Table 1 and Fig. 2A-C). PV-loops demonstrated improved myocardial contractility with increased dp/dt_{max} (preload-dependent) and Ees (preload-independent) as well as improvements in the systolic parameters SV and SW in *AAV9/ βARKct*-treated *mdx* mice (Table 1, Fig. 2A and B). Furthermore, fractional shortening (FS) in echocardiography was increased in *AAV9/ βARKct*-treated *mdx* mice compared to untreated *mdx* mice (Table 1, Fig. 2C). Echocardiographic analyses of *Sgcd-/-* mice showed a significant increase in FS after *AAV9/ βARKct* treatment compared with untreated animals and a trend towards an increased dp/dt_{max} and Ees (Fig. 2, Table 1). In *mdx* and *Sgcd-/-* mice, PV loops showed diastolic dysfunction with impaired active (low Tau and dP/dt_{min}) and passive relaxation (EDP only in *Sgcd-/-* mice), which remained unchanged after treatment with *AAV9/βARKct* (Table 1). In the examined mouse models βARKct has obviously no effects on loading conditions as afterload measured by arterial elastance (E_a) does not differ between the groups. In parallel to the improved left ventricular function, cardiac expression of βARKct resulted in a significantly lower cardiac expression of brain-natriuretic peptide (BNP) mRNA expression in *mdx* mice (Fig. 2D). In contrast to *mdx* mice, cardiac BNP mRNA expression in *Sgcd-/-* mice was not different from wild type mice and there were no changes after treatment with βARKct (Fig. 2D).

3.3. *Attenuation of myocardial hypertrophy in* mdx *mice*

In echocardiography significant hypertrophy compared to wildtype mice can already be detected in 6-month-old *mdx* mice (supplemental Figure 1, Table 1). At the age of 12 months *mdx* mice revealed hypertrophic cardiomyopathy

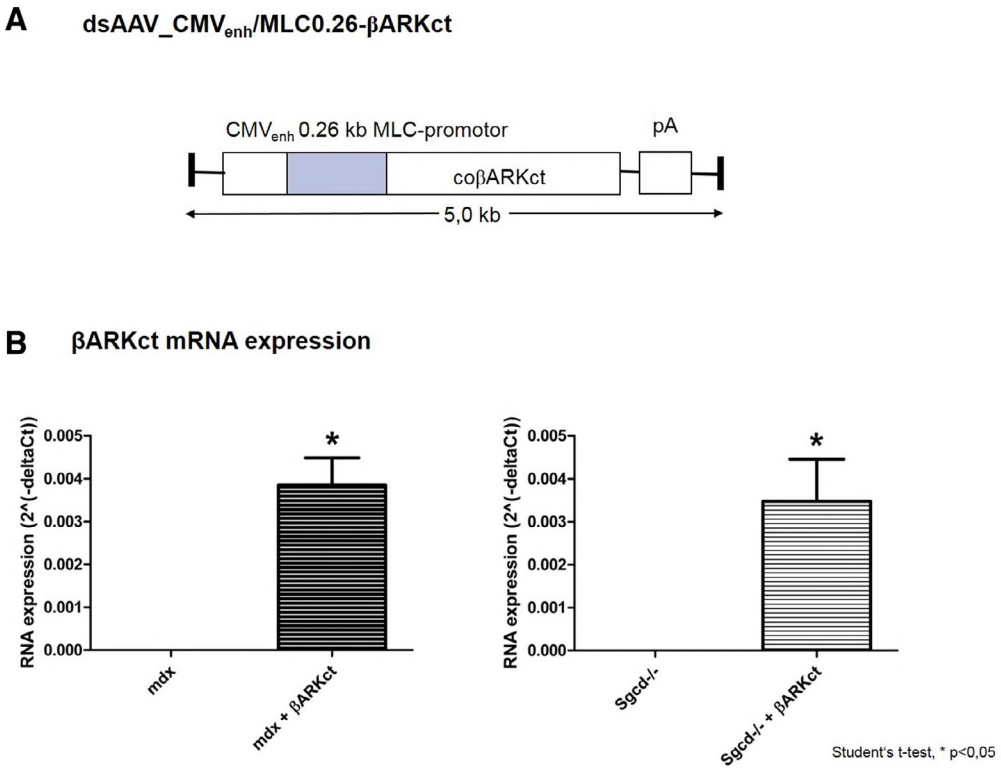

Fig. 1. Long-term cardiac βARKct transgene expression in mdx and Sgcd-/- mice.
(A) Schematic presentation of the double-stranded AAV9 genome plasmid (*AAV9/βARKct*) carrying a codon-optimized βARKct-cDNA (coβARKct) under transcriptional control of a CMV-enhanced (CMV_{enh}), 0,26 kb myosin light chain (MLC0.26) promoter. (B) RT-PCR showed an showed a similar expression of *βARKct* mRNA in 12 months-old *AAV9/βARKct*- treated *mdx* and 12 months-old *AAV9/βARKct*-treated *Sgcd-/-* mice compared to untreated control mice ($n = 8$ each animal group) (student's *t*-test, $^*p < 0{,}05$).

with increased enddiastolic posterior-wall-thickness (PWTd) in echocardiography, significant increase of cardiac cell size as assessed by cell surface area measurements and a higher heart-to-body weight ratio (mg/g) compared to age-matched wild type mice (Table 1 and Fig. 3). Chronic gene transfer of *AAV9/ βARKct* into *mdx* mice resulted in an attenuation of PWTd, smaller cardiomyocytes and lower heart-to-body-weight ratio compared to untreated *mdx* mice (Fig. 3A–C).

In contrast to *mdx* mice, *Sgcd-/-* mice revealed subtle left ventricular dilatation with slightly increased EDV and discrete myocardial hypertrophy as indicated by a higher heart-to body weight ratio and slightly increased cardiomyocyte size compared to wild type controls (Table 1 and Fig. 3).

Treatment with *AAV9/βARKct* had no positive effects on myocardial hypertrophy in *Sgcd-/-* mice. Interestingly, we found subtle hints for aggravation of cardiac hypertrophy in *AAV9/βARKct*- treated *Sgcd-/-* mice demonstrated by an increased size of cardiomyocytes, whereas heart-to body ratio and PWTD remained unchanged (Fig. 3). However, βARKct-gene transfer has no influence on fibrosis in both *mdx* and *Sgcd-/-* mice (supplemental Figure 3).

3.4. Inhibition of GRK2 by βARKct gene transfer is effective in mdx *but not in* Sgcd-/- *mice*

Upregulation of GRK2 plays a key role in the pathogenesis of heart failure. Therapeutic inhibition through βARKct had positive inotropic effects and reversed adverse ventricular remodelling in heart failure. Immunoblot analysis shows upregulated cardiac GRK2 protein levels in hearts of *mdx* mice compared to wild type controls whereas GRK2-protein levels in *Sgcd-/-* mice are not different from wild type littermates (Fig. 4). In *mdx* mice, treatment with βARKct leads to a reduction of cardiac GRK2-protein levels comparable to those of C57Bl/10 control mice. *AAV9/ βARKct*-treated *Sgcd-/-* mice show cardiac GRK2- protein levels similar to untreated *Sgcd-/-* mice and C57Bl/6 controls. This finding further underlines the hypothesis of substantial differences in the pathogenesis of cardiomyopathies in the two mouse models and may explain stronger beneficial effects of *AAV9/βARKct*-treatment in *mdx* mice compared to *Sgcd-/-* mice. These data suggests that βAR signalling is not a driving force in this cardiomyopathy, which is consistent also with the lack of an effect of β-blockers in this model.

To further analyse effects of *AAV9/ βARKct*-treatment on βAR-signalling we measured cardiac mRNA expression of the stimulatory G protein alpha subunit $G_s\alpha$. As expected for heart failure models, stimulatory $G_s\alpha$ mRNA is down-regulated in hearts of *mdx* and *Sgcd-/-* mice compared to wild type controls (supplemental Figure 4A). *AAV9/ βARKct*-treatment had no effect on $G_s\alpha$ mRNA expression in both mouse models suggesting that there is no significant influence of *AAV9/ βARKct* on adenylyl cyclase (AC)-activity. Furthermore, downstream major components of AC-mediated β-

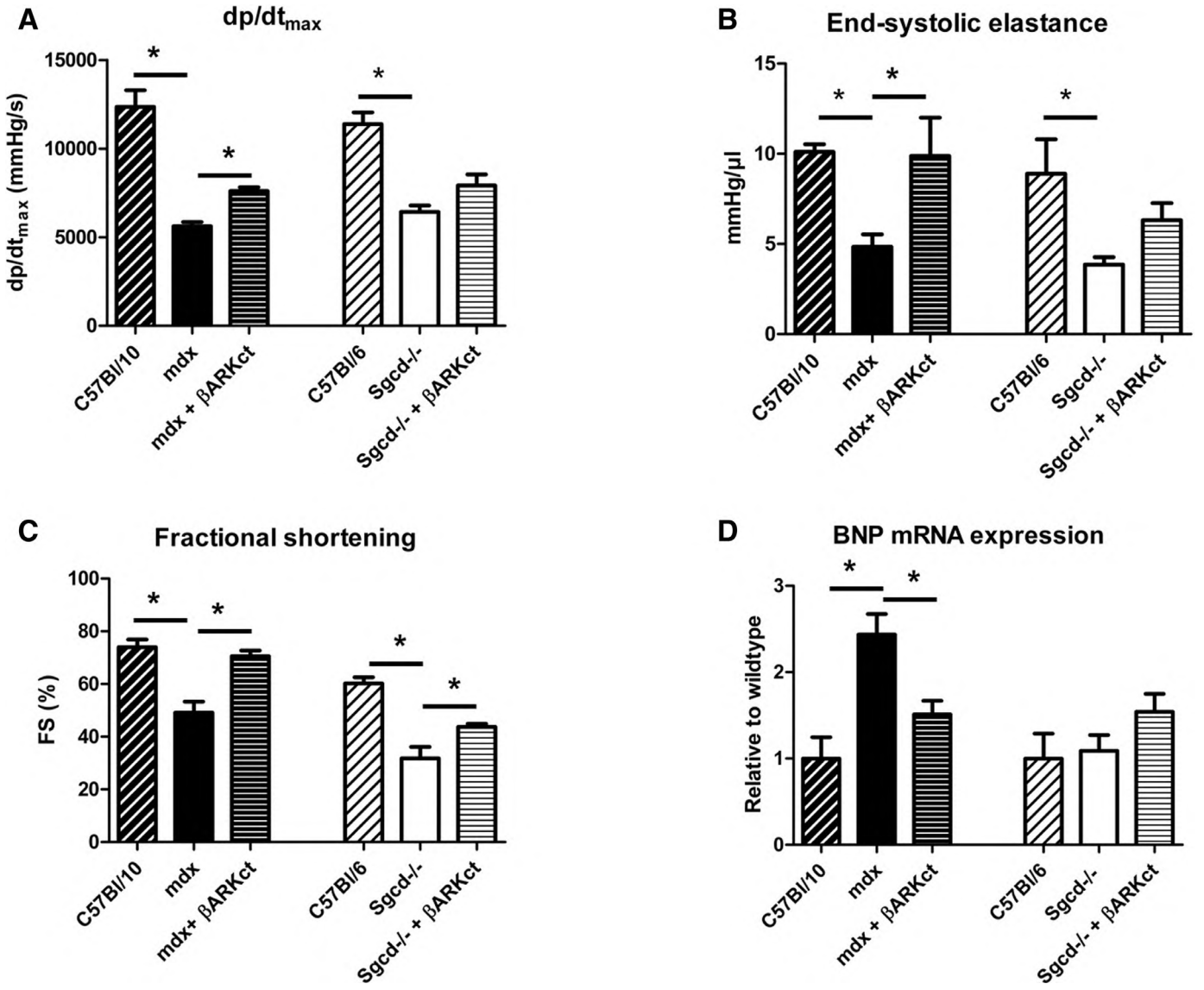

Fig. 2. Cardiac haemodynamics after treatment with AAV9/βARKct.
Animal numbers see Table 1. In 12-month-old *mdx* and *Sgcd-/-* mice impaired myocardial contractility was assessed by measurement of (A) dp/dt_{max}, (B) end-systolic elastance (Ees) and (C) fractional shortening (FS) by PV-loops and echocardiography. (A)–(C) Treatment with *AAV9/βARKct* lead to improved myocardial contractility with higher dp/dt_{max}, Ees and increased FS in *mdx* mice. In *Sgcd-/-* mice the invasively measured parameters for myocardial contractility dp/dt_{max} and Ees remain unchanged. However, FS in echocardiography is increased in both *mdx* and *Sgcd-/-* mice treated with *AAV9/βARKct*. (D) Cardiac BNP expression was significantly increased in 12 months-old untreated *mdx* mice compared to C57Bl/10 control mice (2,4(±0,2)-fold, $^{+}p < 0{,}05$). Treatment with *AAV9/βARKct* significantly reduced cardiac BNP expression in *mdx* mice (2,4(±0,2)- vs. 1,5(±0,2)-fold)). There were no differences in BNP expression between *AAV9/βARKct*-treated *Sgcd-/-* mice, untreated *Sgcd-/-* mice and C57Bl/6 control mice. $^{*}p < 0.05$ one-way ANOVA ($n = 8$ each animal group for BNP analysis).

adrenergic signalling calcium handling were analysed. Levels of cardiac sarcoplasmic reticulum Ca2+-ATPase (SERCA2A) mRNA were downregulated in *mdx* and *Sgcd -/-* mice compared to wildtype mice, however did not change after *AAV9/βARKct*-treatment (supplemental Figure 4B).

3.5. AAV9/ βARKct *reduces activation of NF-kappaB in hearts of* mdx *mice*

Several studies have indicated that activation of the transcription factor nuclear factor kappa-light-chain-enhancer of activated B cells (NFkB), besides modulating inflammation, may play an important role in the development of cardiac hypertrophy and remodelling [24,25]. Similar to cardiac GRK2 protein expression, immunoblot analysis reveals upregulated cardiac protein levels of phosphorylated p65 (pp65) in hearts of *mdx* mice compared to wildtype controls (Fig. 5). In contrast, pp65-protein levels in *Sgcd-/-* mice are not different from wildtype littermates. In accordance to reduced myocardial hypertrophy, *AAV9/ βARKct*-treated *mdx* mice showed significantly lower cardiac pp65 protein levels compared to untreated mice. In conjuction with increased cardiomyocyte

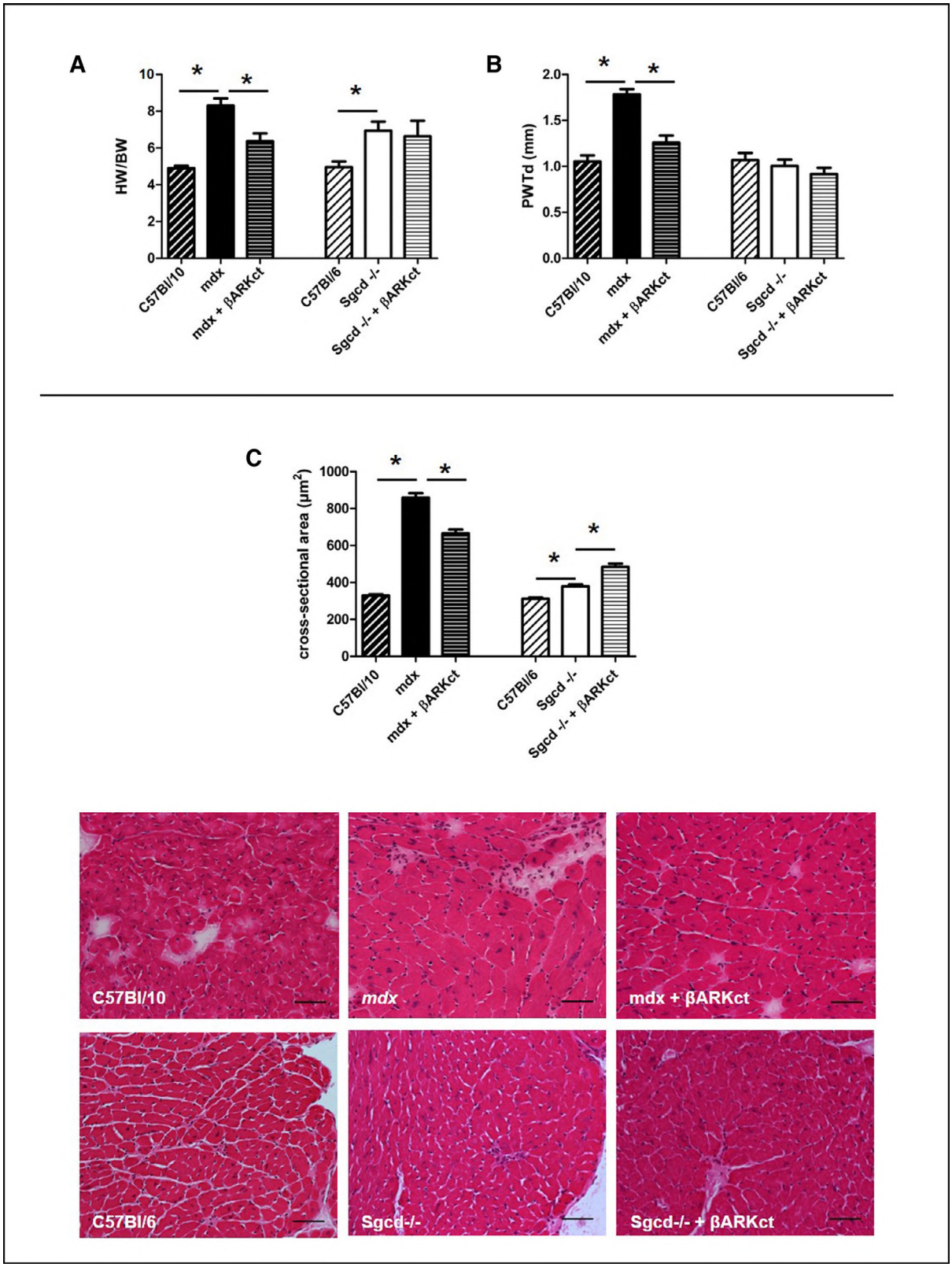

Fig. 3. Attenuation of myocardial hypertrophy in *mdx* but not Sgcd-/- mice after treatment with AAV9/βARKct.
(A) Heart-to bodyweight ratios (HW/BW in mg/g) were increased in both 12-month-old untreated *mdx* and *Sgcd-/-* mice compared to C57Bl/10 and C57Bl/6 control mice. Treatment with *AAV9/βARKct* attenuated the increased HW/BW in *mdx* but not *Sgcd-/-* mice. (B) Diastolic posterior wall thickness (PWTd) was significantly increased in untreated *mdx* mice and could significantly be reduced by *AAV9/βARKct* treatment. No changes were observed in *Sgcd-/-* mice (A+B $n = 10$ to 11). (C) Cardiomyocyte cross-sectional areas were increased in cardiomyocytes from untreated *mdx* and *Sgcd-/-* mice compared to control mice and attenuated *in mdx* but not *Sgcd-/-* mice (each group $n = 5$). (D) Representative cardiac cross-sections from individual groups (20x total magnification). $^{*}p < 0.05$ one-way ANOVA.

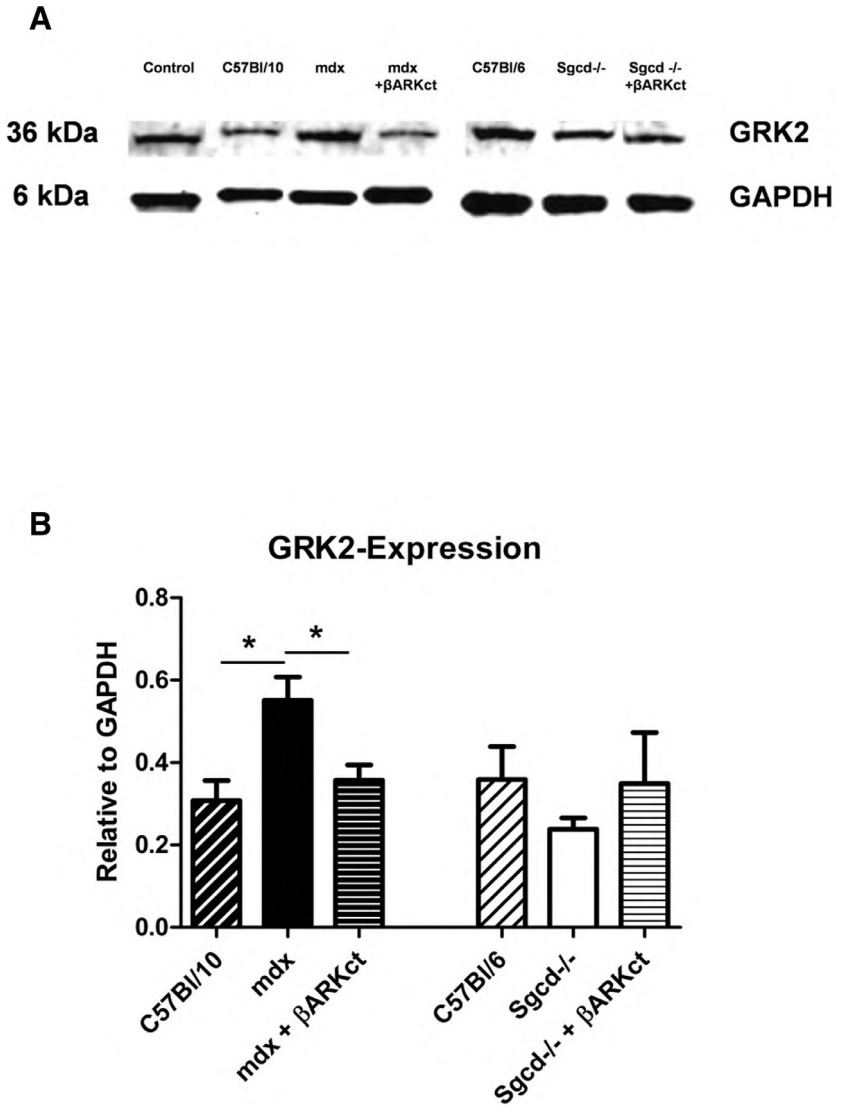

Fig. 4. Different GRK2 expression in *mdx* and *Sgcd-/-* mice.
(A) Representative immunoblots for GRK2 and GAPDH. (B) Quantification of immunoblots for GRK2 relative to GAPDH: Untreated *mdx* mice showed upregulated cardiac GRK2 protein levels compared to C57Bl/10 control mice, which were normalised by treatment with *AAV9/βARKct*. GRK2-protein levels in untreated *Sgcd-/-* mice were not different from C57Bl/6 control mice and there were no changes after *AAV9/βARKct*-treatment in *Sgcd-/-* mice. $N = 5$ for all groups. $^{*}p < 0.05$ one-way ANOVA.

cross-sectional areas representing subtle signs of hypertrophy on the cellular level, the markedly increased pp65 protein levels in hearts of *AAV9/ βARKct*-treated *Sgcd-/-* mice compared to untreated mice, may support its potential role in modulating hypertrophy in these mice.

4. Discussion

Cardiac involvement increasingly determines mortality of patients with muscular dystrophies such as DMD or sarcoglycanopathies like LGMD2F. These muscular dystrophies are characterised by an impaired mechanical interaction of the cytoskeleton and the extra-cellular matrix. β-blocker treatment in mouse models for DMD (*mdx)* and LGMD2F (*Sgcd-/-*) revealed conflicting results. This indicates that despite the close biochemical association between dystrophin and the membrane-bound sarcoglycan complex, therapeutic responses to therapies may differ even between similar cardiomyopathies [7]. In this study we investigate the effectiveness of AAV-mediated cardiac gene transfer of βARKct, a peptide inhibitor of GRK2, on the progression of cardiomyopathy in *mdx* and *Sgcd-/-* mice. Our data show an improvement of cardiac haemodynamics and a reduction of hypertrophy by *AAV9/βARKct* treatment in *mdx* mice, whereas *Sgcd-/-* mice revealed a moderate improvement of left ventricular function (only fractional shortening, but not +dp/dt) and no change in compensatory hypertrophy. These findings are in line with the results observed after β-blocker treatment in these two models [7] and indicate that the response to βARKct-treatment depends on the underlying molecular cause, activated pathways and potentially to the level of adrenergic dysregulation.

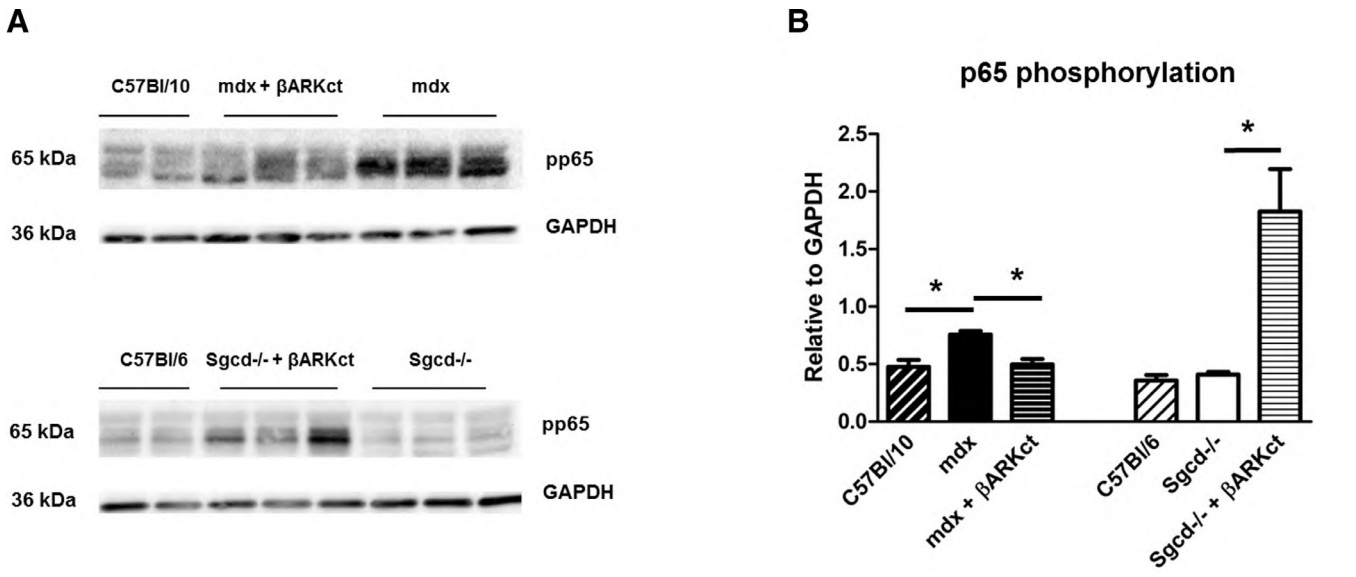

Fig. 5. AAV9/ βARKct reduces activation of NF-kappaB in hearts of *mdx* mice.
(A) Representative Immunoblots for pp65 and GAPDH in heart tissue from experimental groups as indicated on the blot. (B) Quantification of immunoblots for pp65 relative to GAPDH: Untreated *mdx* mice showed upregulated cardiac pp65 protein levels compared to C57Bl/10 control mice. *AAV9/βARKct*-treated *mdx* mice show reduced cardiac protein levels of pp65. Pp65-protein levels in untreated *Sgcd-/-* mice were not different from C57Bl/6 control mice. *AAV9/βARKct*-treatment leads to an overexpression of cardiac pp65-protein levels in *Sgcd-/-* mice. $N = 5$ for all groups. $^{*}p < 0.05$ one-way ANOVA.

In order to further explain the different reponse to *AAV9/βARKct* a closer look on its mode of action might be helpful. Overexpression of GRK2 is considered to play a key role in the pathogenesis of many forms of heart failure and its therapeutic inhibition through βARKct is a promising gene therapy strategy showing beneficial effects in several different animal models [9,13,26]. Restoration of impaired βAR-mediated contractile responsiveness in heart failure has been proposed as a major underlying molecular mechanism for the inotropic effect of βARKct. However, comprehensive cAMP-dependent downstream effects have not yet been determined [27]. Moreover, a previous in vitro study showed that the inotropic effects of βARKct in normal and diseased cardiomyocytes are independent of the classical cAMP-related pathway downstream of activated βARs supporting our finding of missing effects of βARKct on major components of cAMP-mediated calcium handling in both mouse models [28].

It has been shown that stimulation of G$\beta\gamma$ protein-dependent signalling inhibits L-type Ca^{2+} channels (LLC) currents and the G$\beta\gamma$ sequestering peptide βARKct exerts its effects by interruption of this inhibitory pathway [28]. While LLC currents are reduced in *mdx* mice, calcium influx through LLC is even excessive in *Sgcd-/-* mice and disinhibition of LLC currents in cardiomyocytes by βARKct might even exacerbate cardiomyopathy in *Sgcd-/-* mice [29].

Besides Ca^{2+} handling, there are further distinct molecular differences between *mdx* and *Sgcd-/-* mice. Upregulation of GRK2 was only found in *mdx* mice, a fact which may at least partially explain stronger treatment effects of *AAV9/βARKct* in *mdx* mice compared to *Sgcd-/-* mice. This is in line with the data from a previous study showing that beta-adrenergic response of cardiac muscle in *Sgcd-/-* mice is not altered compared to wildtype mice [30].

Another explanation for the different susceptibility to *AAV9/βARKct*-treatment might be well characterized differences in pathomechanisms causing cardiomyopathy in these two models. In *mdx* mice, cardiomyopathy likely develops from membrane instability during contraction with consecutive excessive influx of calcium (Ca^{2+}) in affected cardiomyocytes [31,32]. In *Sgcd-/-* mice the integrity of the sarcoglycan complex is not critical and passive extension-induced membrane damage may not be causal [33,34]. Instead, cardiomyopathy in *Sgcd-/-* mice was explained by vascular constrictions and intermittent ischemic-like events due to vascular dysfunction associated with perturbation of the sarcoglycan-sarcospan complex (SSC) in vascular smooth muscles as well as paracrine effects from diseased cardiomyocytes [35,36].

A further difference between the two models might be the role of NFκB -signalling which plays an important role in the development of cardiac hypertrophy [25,26]. Furthermore, in earlier studies a linkage of enhanced GRK2 expression to myocardial hypertrophy in a pressure overload mouse model and transgenic mice that overexpress an amino-terminal peptide of GRK2 (βARKnt) develop cardiac hypertrophy has been shown [37,38]. A new aspect in the present study may be a interaction of GRK2 with subunits of the transcription factor NFκB-subunits in *mdx* mice, thereby promoting cardiac hypertrophy. A study by Patial et al. demonstrates that overexpression of GRK2 or GRK5 enhances tumor necrosis alpha (TNFalpha)-mediated NFκB-activity suggesting them as important mediators of a non-traditional NFκB-signalling pathway [39].

Mdx mice revealed an increased activity of NFκB (measured as phosphorylation of the subunit p65) while NFκB - activity in hearts of untreated *Sgcd-/-* mice was not altered compared to wildtype. βARKct-treated *mdx* mice were

characterised by reduced phosphorylation of the NFκB subunit p65 associated with improved contractility and reduced myocardial hypertrophy compared to untreated mice. These findings are consistent with a previous study reporting amelioration of pressure-overload induced cardiac hypertrophy due to cardiac specific ablation of the NFκB p65 subunit in mice [26]. Furthermore, it has been shown that cardiac contractile dysfunction in utrophin/dystrophin-deficient mice can be significantly improved by a peptide-based inhibition of NFκB [40].

AAV9/βARKct treatment of *Sgcd-/-* mice was associated with increased phosphorylation of p65 and subtle signs of hypertrophy on the cellular level, which points to the complexity of pathological determinants of cardiomyopathy in different mouse models.

The increased NFκB -activity in *mdx* mice might be triggered by increased intracellular resting Ca^{2+}-levels. Similar to our findings in hearts of *mdx* mice, Altamirano et al. found an elevated transcriptional activity of NFκB in *mdx* skeletal muscle cells and showed that a reduction of intracellular Ca^{2+} reverses activated NFκB – signalling [41]. Furthermore, a reduction or inhibition of p65 was able to ameliorate pathology in skeletal muscles of *mdx* mice [42,43].

A limitation of the study could be the different timing of disease progression in *mdx* and *Sgcd-/-* mice. *Mdx* mice show a cardiac phenotype not before the age of 4 months, whereas in *Sgcd-/-* mice cardiac pathology can be found from the age of 3 months. However, *Sgcd-/-* mice show early histopathology in skeletal muscle partially already at the age of 2 weeks. It is therefore possible that βARKct-treatment has been started at different stages of disease progression between the two models possibly contributing to the different effects of the therapy in these models. *Mdx* and *Sgcd-/-*mice were bred in different genetic backgrounds and may not be directly comparable. To address these limitation *mdx* and *Sgcd-/-*mice were compared to wildtype controls of the same background (C57Bl/10 and C57Bl/6, respectively).

We cannot exclude that systemic effects of anaesthetics may be different in the two background strains and may influence cardiac hemodynamics in pressure-volume loops experiments. However, doses used were similar between the groups and heart rates, representing a similar level of cardiac activation, were not different between the two strains. The trend to lower heart rates in untreated cardiomyopathic *mdx* and *Sgcd-/-*mice rather reflects impaired cardiac function and increased vulnerability to external stress factors in these mice.

Taken together, chronic inhibition of GRK2 through AAV9-mediated cardiac overexpression of βARKct is effective in the *mdx* mouse model of DMD and represents a promising tool to treat cardiomyopathies. However, effectiveness of this therapy may vary between different genetic causes of heart failure, which may involve different pathways and levels of adrenergic dysregulation including GRK2 upregulation. As shown here, even despite the tight functional association of dystrophin and δ-sarcoglycan, the pathomechanisms of cardiomyopathy in *Sgcd-/-* and *mdx* mice are dinstinctly different, which may explain the less beneficial effectiveness following chronic βARKct expression in the heart of *Sgcd-/-* mice.

Funding

P.M., H.A.K. und O.J.M are supported by the DZHK (German Centre for Cardiovascular Research) and by the BMBF (German Ministry of Education and Research). W.J.K. is the W.W. Smith Chair in Cardiovascular Medicine and supported by National Institute of Health (NIH) grants R37 HL061690, P01 HL108806 (Project 3), and P01 HL075443 (Project 2).

Acknowledgements

The authors thank Barbara Leuchs and the German Cancer Research Center (DKFZ) vector core production unit for their support in generating AAV vector stocks and Ulrike Gärtner, University of Heidelberg, for expert assistance in animal experiments. We further thank Prof. Dr. Rainer Fink (Institut of Physiology, University of Heidelberg) for providing *mdx* mice and the Nikon Imaging Center for support with microscopy.

Supplementary material

Supplementary material associated with this article can be found, in the online version, at doi:10.1016/j.nmd.2018.12.006.

References

[1] Muntoni F. Cardiomyopathy in muscular dystrophies. Curr Opin Neurol 2003;16:577–83.
[2] Heydemann A, McNally EM. Consequences of disrupting the dystrophin-sarcoglycan- complex in cardiac and skeletal myopathy. Trends Cardiovasc Med 2007;17:55–9.
[3] Rockman HA, Koch WJ, Lefkowitz RJ. Seven-transmembrane-spanning receptors and heart function. Nature 2002;415:206–12.
[4] Huang ZM, Gold JI, Koch WJ. G protein-coupled receptor kinases in normal and failing myocardium. Front Biosci 2011;17:3057–60.
[5] Bristow MR. Beta-adrenergic receptor blockade in chronic heart failure. Circulation 2000;101:558–69.
[6] Jefferies JL, Eidem BW, Belmont JW, Craigen WJ, Ware SM, Fernbach SD, Neish SR, Smith EO, Towbin JA. Genetic predictors and remodeling of dilated cardiomyopathy in muscular dystrophy. Circulation 2005;112:2799–804.
[7] Bauer R, Blain A, Greally E, Bushby K, Lochmüller H, Laval S, Straub V, MacGowan GA. Intolerance to β-blockade in mouse model of delta-sarcoglycan deficient muscular dystrophy cardiomyopathy. Eur J H Fail 2010;12:1163–70.
[8] Harding VB, Jones LR, Lefkowitz RJ, Koch WJ, Rockman HA. Cardiac beta ARK1 inhibition prolongs survival and augments beta blocker therapy in a mouse model of severe heart failure. Proc Natl Acad Sci U. S. A 2001;98:5809–14.
[9] Reinkober J, Tscheschner H, Pleger ST, Most P, Katus HA, Koch WJ, Raake PW. Targeting GRK2 by gene therapy for heart failure: benefits above β-blockade. Gene Therapy 2012;19:686–93.
[10] Rockman HA, Chien KR, Choi DJ, Iaccarino G, Hunter JJ, Ross J Jr, Lefkowitz RJ, Koch WJ. Expression of a beta-adrenergic receptor kinase 1 inhibitor prevents the development of myocardial failure in gene-targeted mice. Proc Natl Acad Sci U S A 1998;95:7000–5.

[11] Schutzer WE, Xue H, Reed J, Oyama T, Beard DR, Anderson S, Mader SL. Age-related β-adrenergic receptor-mediated vasorelaxation is changed by altering G protein receptor kinase 2 expression. Vascul Pharmacol 2011;55(5–6):178–88.

[12] Lymperopoulos T, Rengo G, Funakoshi H, Eckhart AD, Koch WJ. Adrenal GRK2 upregulation mediates sympathetic overdrive in heart failure. Nat Med 2007;13:315–23.

[13] Raake PWJ, Schlegel P, Ksienzyk J, Reinkober J, Barthelmes J, Schinkel S, Pleger S, Mier W, Haberkorn U, Katus HA, Koch WJ, Most P, Müller OJ. AAV6.βARKct cardiac gene therapy ameliorates cardiac function and normalizes the catecholaminergic axis in a clinically relevant large animal heart failure model. Eur Heart J 2013;34(19):1437–47.

[14] Rengo G, Lymperopoulos A, Zincarelli C, Donniacuo M, Soltys S, Rabinowitz JE, Koch WJ. Myocardial adeno-associated virus serotype 6-betaARKct gene therapy improves cardiac function and normalizes the neurohormonal axis in chronic heart failure. Circulation 2009;119(1):89–98.

[15] Goehringer C, Rutschow D, Bauer R, Schinkel S, Weichenhan D, Bekeredjian R, Straub V, Kleinschmidt JA, Katus HA, Müller OJ. Prevention of cardiomyopathy in delta-sarcoglycan knockout mice after systemic transfer of targeted adeno-associated viral vectors. Cardiovasc Res 2009;82:404–10.

[16] Schinkel S, Bauer R, Bekeredjian R, Stucka R, Rutschow D, Lochmüller H, Kleinschmidt JA, Katus HA, Müller OJ. Long-term preservation of cardiac structure and function after adeno-associated virus serotype 9-mediated microdystrophin gene transfer in mdx mice. Hum Gene Ther 2012;23(6):566–75.

[17] Müller OJ, Leuchs B, Pleger ST, Grimm D, Franz WM, Katus HA, Kleinschmidt JA. Improved cardiac gene transfer by transcriptional and transductional targeting of adeno-associated viral vectors. Cardiovasc Res 2006;70:70–8.

[18] Müller OJ, Schinkel S, Kleinschmidt JA, Katus HA, Bekeredjian R. Augmentation of AAV-mediated cardiac gene transfer after systemic administration in adult rats. Gene Ther 2008;15(23):1558–65.

[19] Gao GP, Alvira MR, Wang L, Calcedo R, Johnston J, Wilson JM. Novel adeno-associated viruses from rhesus monkeys as vectors for human gene therapy. Proc Natl Acad Sci U S A 2002;99(18):11854–9.

[20] Dubielzig R, King JA, Weger S, Kern A, Kleinschmidt JA. Adeno-associated virutype 2 protein interactions: formation of pre-encapsidation complexes. J Virol 1999;73(11):8989–98.

[21] Jungmann A, Leuchs B, Rommelaere J, Katus HA, Müller OJ. Protocol for efficient generation and characterization of adeno-associated viral vectors. Hum Gene Ther Methods 2017;28(5):235–46.

[22] Helms SA, Azhar G, Zuo C, Theus SA, Bartke A, Wei JY. Smaller cardiac cell size and reduced extra-cellular collagen might be beneficial for hearts of Ames dwarf mice. Int J Biol Sci 2010;6(5):475–90.

[23] Bauer R, MacGowan GA, Blain A, Bushby K, Straub VW. Steroid treatment causes deterioration of myocardial function in the delta-sarcoglycan-deficient mouse model for dilated cardiomyopathy. Cardiovasc Res 2008;79:652–61.

[24] Kawamura N, Kubota T, Kawano S, Monden Y, Feldman AM, Tsutsui H, Takeshita A, Sunagawa K. Blockade of NF-kappaB improves cardiac function and survival without affecting inflammation in TNF-alpha-induced cardiomyopathy. Cardiovasc Res 2005;66(3):520–9.

[25] Liu Q, Chen Y, Auger-Messier M, Molkentin JD. Interaction between NFκB and NFAT coordinates cardiac hypertrophy and pathological remodeling. Circ Res 2012;110(8):1077–86.

[26] Rengo G, Lymperopoulos A, Zincarelli C, Femminella G, Liccardo D, Pagano G, de Lucia C, Cannavo A, Gargiulo P, Ferrara N, Perrone Filardi P, Koch W, Leosco D. Blockade of β-adrenoceptors restores the GRK2-mediated adrenal $\alpha(2)$ -adrenoceptor-catecholamine production axis in heart failure. Br J Pharmacol 2012;166:2430–40.

[27] Vinge LE, Raake PW, Koch WJ. Gene therapy in heart failure. Circ Res 2008;102:1458–70.

[28] Völkers M, Weidenhammer C, Herzog N, Qiu G, Spaich K, von Wegner F, Peppel K, Müller OJ, Schinkel S, Rabinowitz JE, Hippe HJ, Brinks H, Katus HA, Koch WJ, Eckhart AD, Friedrich O, Most P. The inotropic peptide βARKct improves βAR responsiveness in normal and failing cardiomyocytes through G($\beta\gamma$)-mediated L-type calcium current disinhibition. Circ Res 2011;108(1):27–39.

[29] Cohn RD, Durbeej M, Moore SA, Coral-Vazquez R, Prouty S, Campbell KP. Prevention of CMP in mouse models lacking the smooth muscle sarcoglycan-sarcospan complex. J Clin Invest 2001;107(2):R1–7.

[30] Milani-Nejad N, Schultz EJ, Slabaugh JL, Janssen PM, Rafael–Fortney JA. Myocardial contractile dysfunction is present without histopathology in a mouse model of Limb-Girdle muscular dystrophy-2F and Is prevented after claudin-5 virotherapy. Front Physiol 2016;7:539.

[31] Kamogawa Y, Biro S, Maeda M, Setoguchi M, Hirakawa T, Yoshida H, Tei C. Dystrophin-deficient myocardium is vulnerable to pressure overload in vivo. Cardiovasc Res 2001;50:509–15.

[32] Danialou G, Comtois AS, Dudley R, Karpati G, Vincent G, Des Rosiers C, Petrof BJ. Dystrophin-deficient cardiomyocytes are abnormally vulnerable to mechanical stress-induced contractile failure and injury. FASEB J 2001;15:1655–7.

[33] Hack AA, Cordier L, Shoturma DI, Lam MY, Sweeney HL, McNally EM. Muscle degeneration without mechanical injury in sarcoglycan deficiency. Proc Natl Acad Sci U S A 1999;96:10723–8.

[34] Townsend D, Yasuda S, McNally E, Metzger JM. Distinct pathophysiological mechanisms of CMP in hearts lacking dystrophin or the sarcoglycan complex. FASEB J 2011;25(9):3106–14.

[35] Coral-Vazquez R, Cohn RD, Moore SA, Hill JA, Weiss RM, Davisson RL, Straub V, Barresi R, Bansal D, Hrstka RF, Williamson R, Campbell KP. Disruption of the sarcoglycan- sarcospan complex in vascular smooth muscle: a novel mechanism for CMP and muscular dystrophy. Cell 1999;98:465–74.

[36] Wheeler MT, Allikian MJ, Heydemann A, Hadhazy M, Zarnegar S, McNally EM. Smooth muscle cell-extrinsic vascular spasm arises from cardiomyocyte degeneration in sarcoglycan-deficient cardiomyopathy. J Clin Invest 2004;113(5):668–75.

[37] Choi DJ, Koch WJ, Hunter JJ, Rockman HA. Mechanism of beta-adrenergic receptor desensitization in cardiac hypertrophy is increased beta-adrenergic receptor kinase. J Biol Chem 1997;272:17223–9.

[38] Keys JR, Greene EA, Cooper CJ, Naga Prasad SV, Rockman HA, Koch WJ. Cardiac hypertrophy and altered beta-adrenergic signaling in transgenic mice that express the amino terminus of beta-ARK1. Am J Physiol Heart Circ Physiol 2003;285:H2201–11.

[39] Patial S, Luo J, Porter KJ, Benovic JL, Parameswaran N. G-protein-coupled-receptor kinases mediate TNFα-induced NFκB signalling via direct interaction with and phosphorylation of IκBα. Biochem J 2009;425:169–78.

[40] Delfín DA, Xu Y, Peterson JM, Guttridge DC, Rafael-Fortney JA, Janssen PM. Improvement of cardiac contractile function by peptide-based inhibition of NF-κB in the utrophin/dystrophin-deficient murine model of muscular dystrophy. J Transl Med 2011;9:68.

[41] Altamirano F, López JR, Henríquez C, Molinski T, Allen PD, Jaimovich E. Increased resting intracellular calcium modulates NF-κB-dependent inducible nitric-oxide synthase gene expression in dystrophic mdx skeletal myotubes. J Biol Chem 2012;287(25):20876–87.

[42] Acharyya S, Villalta SA, Bakkar N, Bupha-Intr T, Janssen PM, Carathers M, Li ZW, Beg AA, Ghosh S, Sahenk Z, Weinstein M, Gardner KL, Rafael-Fortney JA, Karin M, Tidball JG, Baldwin AS, Guttridge DC. Interplay of IKK/NF-kappaB signaling in macrophages and myofibers promotes muscle degeneration in Duchenne muscular dystrophy. J Clin Invest 2007;117(4):889–901.

[43] Tang Y, Reay DP, Salay MN, Mi MY, Clemens PR, Guttridge DC, Robbins PD, Huard J, Wang B. Inhibition of the IKK/NF-κB pathway by AAV gene transfer improves muscle regeneration in older mdx mice. Gene Ther 2010;17(12):1476–83.